Visible light-driven Cu(II)-$(Sr_{1-y}Na_y)(Ti_{1-x}Mo_x)O_3$ photocatalysts based on the conduction band control and surface ion modification

Xiaoqing Qiu, Masahiro Miyauchi,* Huogen Yu, Hiroshi Irie *and* Kazuhito Hashimoto*

National Institute of Advanced Industrial Science and Technology, Tsukuba Central 5, 1-1-1 Higashi, Tsukuba, Ibaraki 305-8565, Japan. Research Center for Advanced Science and Technology, The University of Tokyo, 4-6-1 Komaba, Meguro-ku, Tokyo 153-8904, Japan. Graduate School of Engineering, The University of Tokyo, 7-3-1 Hongo, Bunkyo-ku, Tokyo 113-8656, Japan. Clean Energy Research Center, University of Yamanashi, 4-3-11 Takeda, Kofu, Yamanashi 400-8511, Japan.

*Corresponding author: m-miyauchi@aist.go.jp hashimoto@light.t.u-tokyo.ac.jp

Supporting Online Materials

1 Elemental analysis

Table S1. The Composition of the sample derived from ICP and atomic absorption spectrophotometer analysis

Sample	$(Sr_{1-y}Na_y)(Ti_{1-x}Mo_x)O_3$					
	I	II	III	IV	V [b]	VI [c]
Mo content (x) [a]	0 (0)	0.25% (0.25%)	0.9% (1%)	2.0% (2.5%)	1.8% (2.5%)	1.9 % (2.5%)
Na content (y)	0	0.06%	0.16%	0.25%	0.7%	0
Molar ratio (Ti/Sr)	1.07	1.06	1.06	1.05	1.03	1.06

[a] the values given in parentheses are the initial ones.

[b] the sample obtained by the control experiment I

[c] the sample obtained by the control experiment II

Even though, Na and Mo co-doped $SrTiO_3$ samples with the molar ratio Na/Mo = 2 were not obtained. It is clear that the Na content in Sample V was greatly enchanced, compared to Sample IV, if 10 g NaCl was used as the addtional Na source. The sample free of Na was also obtained by using MoO_3 as starting material instead of $NaMoO_4$. Furthermore, the Mo contents in Sample V and VI were very close to that of Sample IV. The XRD patterrns show that Sample V and VI were a single phase

with cubic perovskite structure (not shown). In other words, to a certain extent, the Na contents can be well controlled in the samples with a fixed Mo content, which provides the good oppotunity to study the effects of Na ions on the photocatalytic activities.

2. XRD

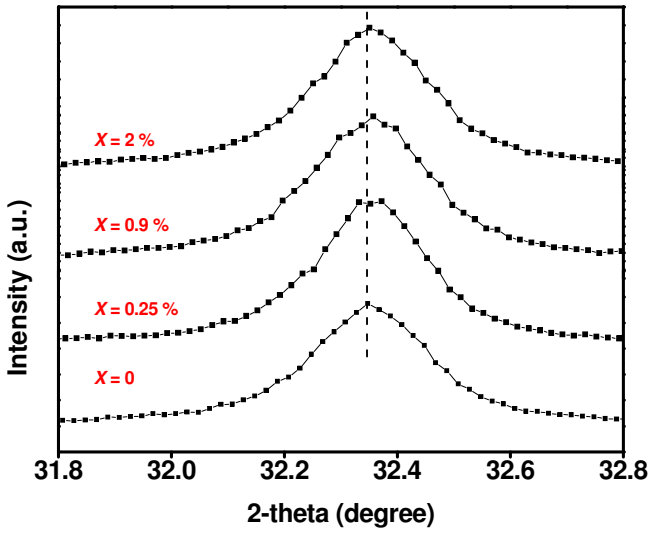

Figure S1. The enlarged peak (110) for $(Sr_{1-y}Na_y)(Ti_{1-x}Mo_x)O_3$ at x = 0, 0.25%, 0.9%, and 2.0%.

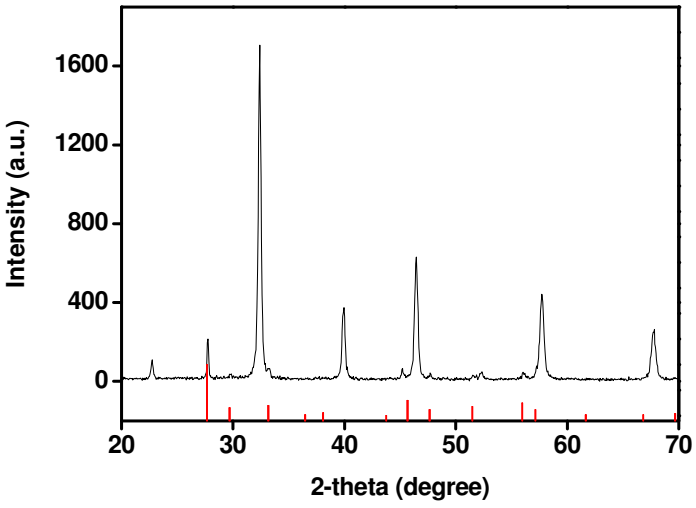

Figure S2. The XRD patterns of $(Sr_{1-y}Na_y)(Ti_{1-x}Mo_x)O_3$ at x = 5%. Vertical bars below the patterns represent the standard diffraction data from JCPDS file for bulk $SrMoO_4$ (No. 08-0482)

3. TEM

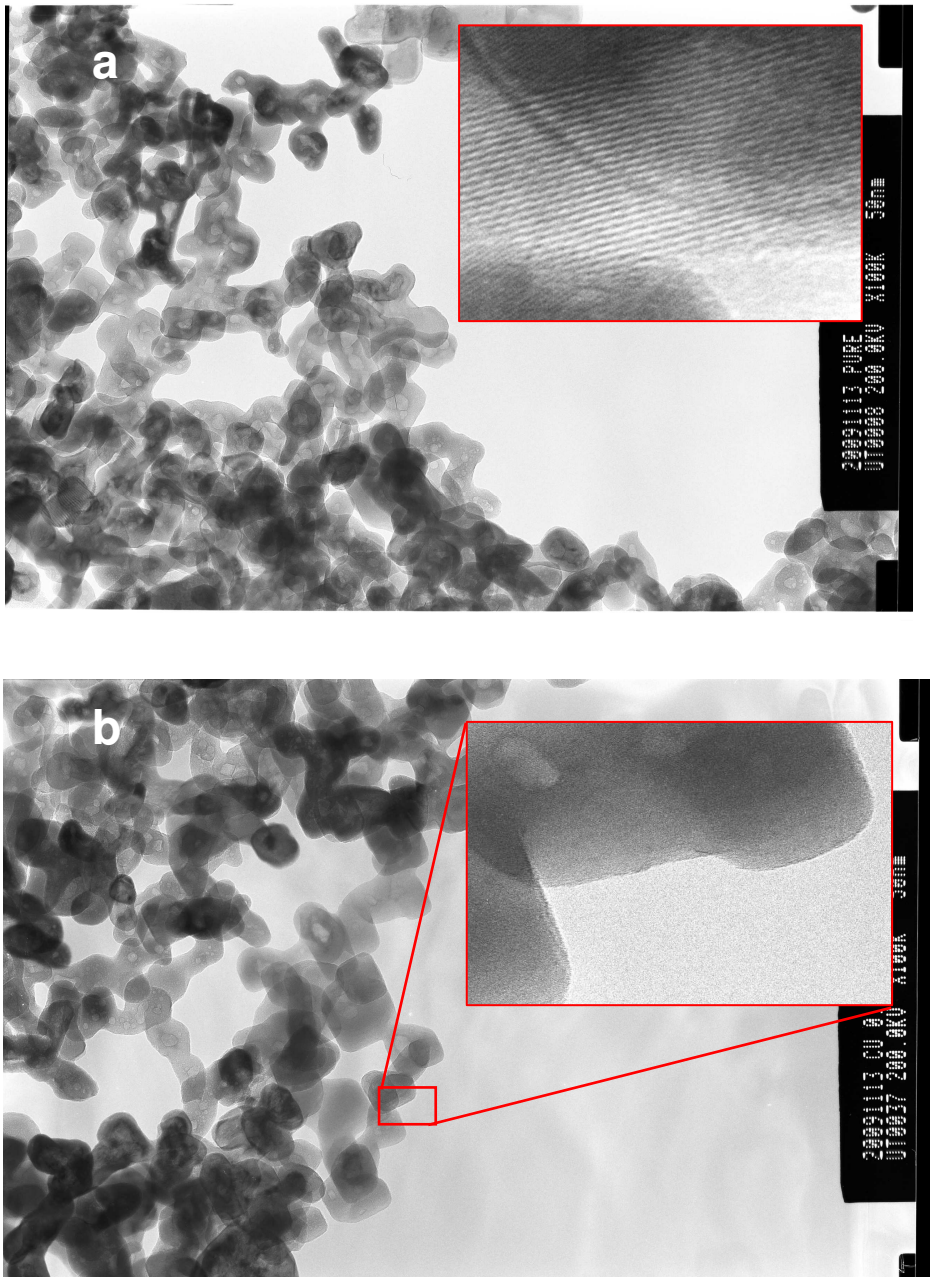

Figure S3. TEM images of a) non-doped $SrTiO_3$ (a), and b) Cu(II)- $SrTiO_3$

4. XPS

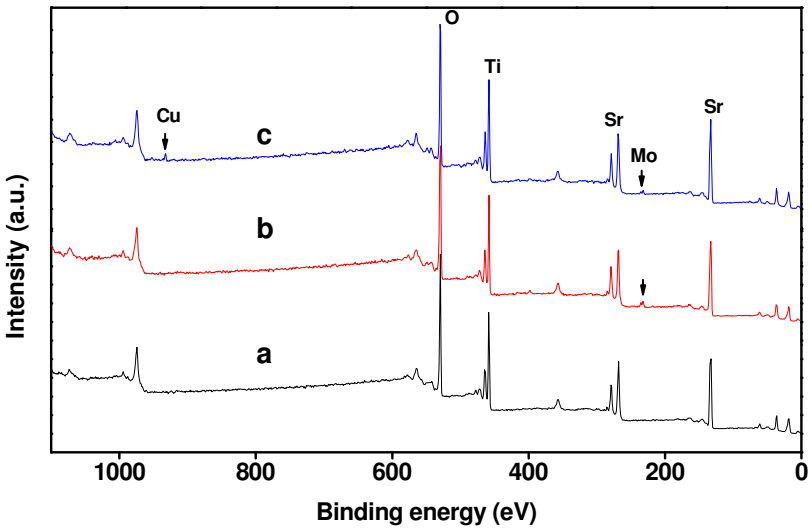

Figure S4. Full-scale XPS spectra of samples. (a) non-doped $SrTiO_3$, (b) $(Sr_{1-y}Na_y)(Ti_{1-x}Mo_x)O_3$ at $x = 2.0$ %, (c) Cu(II)-$(Sr_{1-y}Na_y)(Ti_{1-x}Mo_x)O_3$ at $x = 2.0$ %.

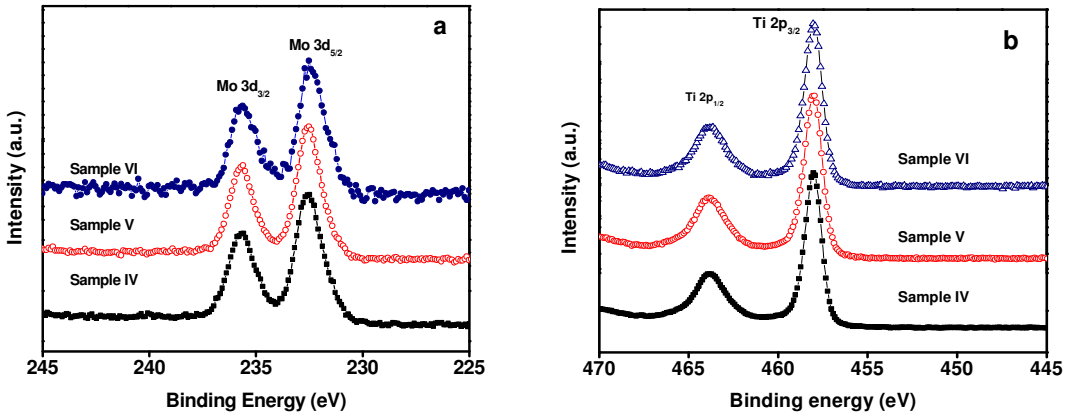

Figure S5. (a) Mo 3d core-level spectra of Sample IV, V and VI, (b) Ti 2p core-level spectra of Sample IV, V and VI.

There is no obvious difference in the chemical states of elements Mo and Ti in the Sample V and VI, compared to Sample IV.

5. UV-vis spectra

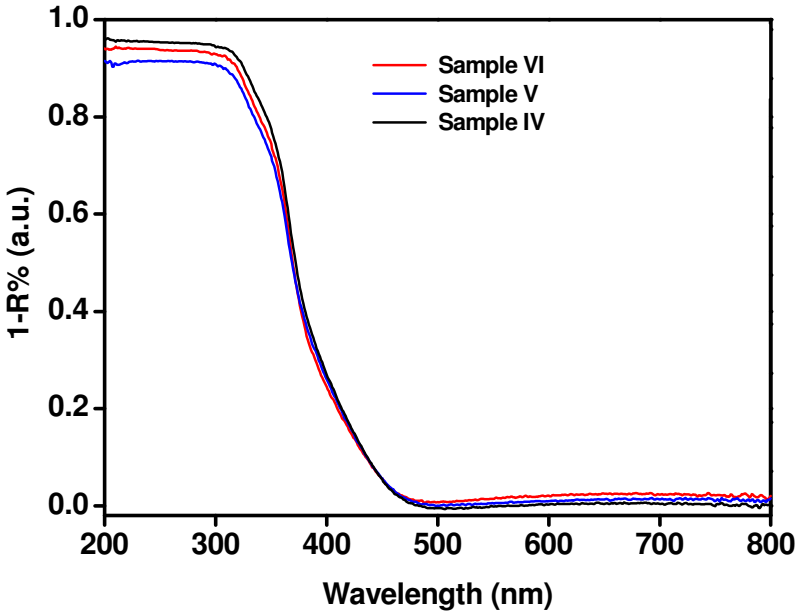

Figure S6a . UV-visible absorption spectra of Sample IV, V and VI.

The overlapping absorption edges of Sample IV, V and VI evidence their similar optical properties. This is because the Mo contents are comparable to each other

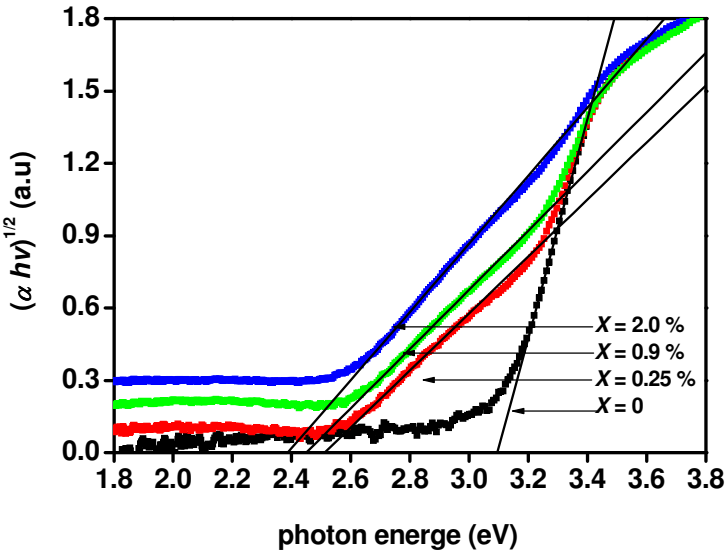

Figure S6b. The relationships between $(ahv)^{1/2}$ and photon energy of

$(Sr_{1-y}Na_y)(Ti_{1-x}Mo_x)O_3$ at x = 0, 0.25 %, 0.9 %, and 2.0 %, respectively.

.

$SrTiO_3$ is an indirect gap semiconductor. [Koffyberg, F. P.; Dwight, K.; Wold, A. *Solid State Commun.* **1979**, *30*, 433.] The optical band gap energies (Eg) were calculated from the estimated from the corresponding absortption spectra by extrapolation of the linear portion of the $(\alpha hv)^{1/2}$ curve versus the photon energy hv to $(\alpha hv)^{1/2}$ = 0. As illustrated in the inset of Figure 6b, the band gap values are determined to be approximately 3.10, 2.52, 2.45, and 2.38 eV for $(Sr_{1-y}Na_y)(Ti_{1-x}Mo_x)O_3$ samples at x = 0, 0.25%, 0.9%, and 2.0%, respectively. From the DOS calculations, the change of the valence band position is ignored, then the decrease of the conduction band position could be estimated by change of the band gap energies. For example, the change of the CB position is approximately 0.7 eV for the $(Sr_{1-y}Na_y)(Ti_{1-x}Mo_x)O_3$ samples at x = 2 % compared to that of $SrTiO_3$.

6. BET

Table S2. Specific Surface Area Values

Sample	I (x = 0)		II (x= 0.25%)		III (x = 0.9%)		IV (x= 2.0%)		V (x= 1.8%)		VI (x= 1.9%)	
	Bare	With Cu(II)	Bare	With Cu(II)	Bare	With Cu(II)	Bare	With Cu(II)	Bare	With Cu(II)	Bare	With Cu(II)
S_{BET} (m^2/g)	24.3	25.3	22.8	23.7	26.2	27.3	24.7	26.5	20.4	21.2	24.6	25.4

All the samples had comparable specific surface areas. So, it can not account for the enhancement of the photocatalytic activities upon Cu(II) modifaction and Mo^{6+} as well as Na^+ doping..

7. Irradiation light source

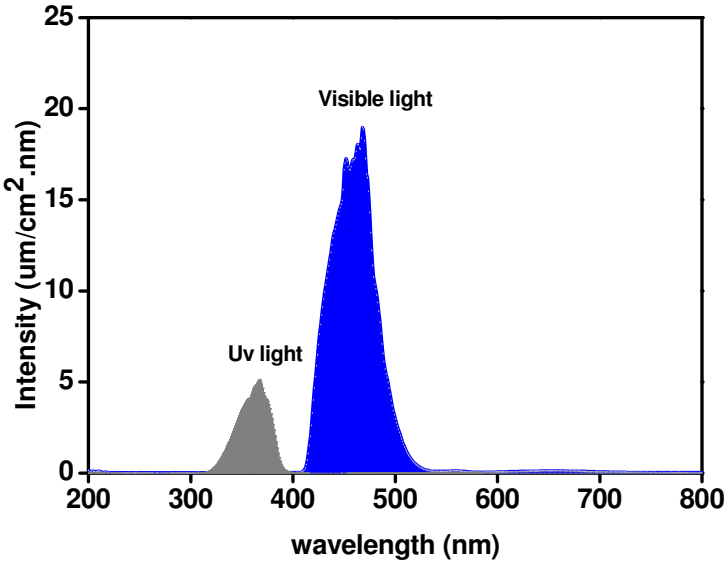

Figure S7. the light source for the visible light irradaition and UV irradiation

The wavelength of visible light is from 400 to 530 nm, and the light intensity is 1 mW/cm^2. The UV light intensity was calibrated to control the same absorbed photon numbers as that of Cu(II)-($Sr_{1-y}Na_y$)($Ti_{1-x}Mo_x$)O_3 at x = 2.0% under visible light irradiation.

8. Photocatalytic activity

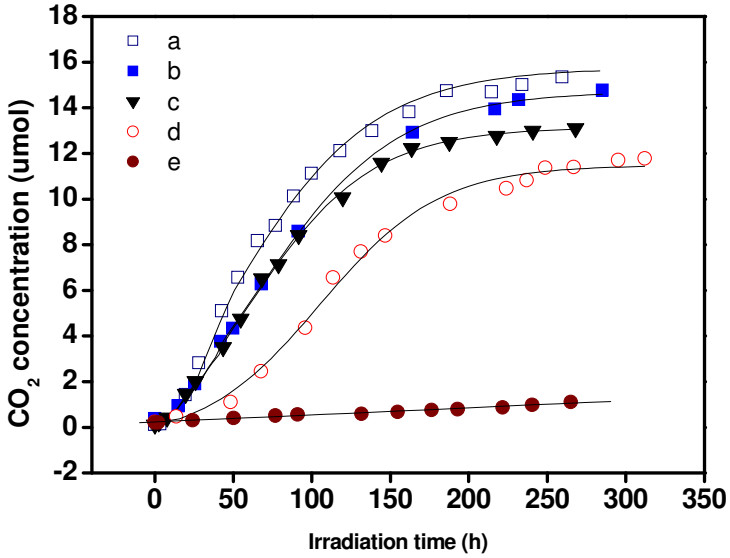

Figure S8.. Comparative studies of CO_2 generation over different samples under visible light irradiation. a) Cu(II) modfied Sample IV, i.e. Cu(II)-$(Sr_{1-y}Na_y)(Ti_{1-x}Mo_x)O_3$ at x = 2.0% in the main text, b) Cu(II)-$(Sr_{1-y}Na_y)(Ti_{1-x}Mo_x)O_3$ at x = 5%, i. e. Cu(II) modified the sample with mirnor impurity of $SrMoO_4$. c) Cu(II) modfied Sample V obtained by the control experiment I using NaCl as additional Na^+ source, d) Cu(II) modfied Sample VI obtained by the control experiment II using MoO_3 as dopant source, e) Cu(II)-MoO_3.

The highest photocatalytic activity was obtained over Cu(II)-$(Sr_{1-y}Na_y)(Ti_{1-x}Mo_x)O_3$ at x = 2.0 % (curve a). Further increasing the Mo content, the activity slightly decreased (curve b), due to the negative effects of impurtiy $SrMoO_4$ on the visible light activity. Concerning the relatively low Na contents in the samples, parallel experiments were performed under identical condition to get the various Na contents in the samples with a fixed Mo content to explore the effects on Na on the photocatalytic activities. By using NaCl as an additional Na source or MoO_3 as starting materials, the Na contents in the samples were successfully controlled. Our $SrTiO_3$ co-doped with Mo and Na sample exhibits the better activity than $SrTiO_3$ doped with Mo alone. But the activity decreased with the further increasing of Na content in the sample. One possible reason

for this is that Na ions are in favor of co-doping in $SrTiO_3$, and is not effective for the photocatalytic activity.[A. Fernandez, G. Lassaletta, V. M. Jimenez, A. Justo, A. R. Gonazalez-Elipe, J. M. Herrmann, H. Tahiri, Y. Ait-Ichou, *Appl. Cata. B* 1995, 7, 49. b] A. Fujishima, T. N. Rao, D. A. Tryk, *Electrochim. Acta* 2000, 45, 4683.] In the present study, optimum doping densities for Mo^{6+} and Na^+ were 2.0 % and 0.25 %, respectively.

9. Details for the calculations of quantum efficiency

The calculation of quantum efficiency (QE) was conducted using the same procedure reported in the literatures [H. Irie, Y. Watanabe, K. Hashimoto, *J. Phys. Chem. B* 2003, 107, 5483. H. Irie, S. Miura, K. Kamiya, K. Hashimoto, *Chem. Phys. Lett.* 2008, 457, 202.].

Take Cu(II)-$(Sr_{1-y}Na_y)(Ti_{1-x}Mo_x)O_3$($x$ = 2.0%) for example. Under the visible light irradiation, the wavelength of visible light is from 400 to 530 nm, and the light intensity is 1 mW/cm^2. The irradiating area is 5.5 cm^2. Therefore, the absorption rate of incident photons (R_p^a) was determined to be 1.02×10^{15} quanta·sec^{-1}. As for CO_2 generation, assuming that the reaction from IPA to CO_2 is proceeded: $C_3H_8O + 5H_2O + 18h^+ \rightarrow 3CO_2 + 18H^+$, that is, six photons are required to produce one CO_2 molecule. The CO_2 generation rate (R_{CO_2}) was obtained from the slope of the CO_2 generation curve between the irradiation time of ca. 10 to 70 h in Figure S12. Using the conventional least-squares method, R_{CO_2} was determined to be 0.148 μmol·h^{-1} (i.e, 2.47×10^{13} qunta.sec^{-1}). Thus the QE for CO_2 generations were calculated using the following equation: $QE = R_p^r / R_p^a = 6R_{CO_2} / R_p^a$

QE = $6 \times 2.47 \times 10^{13}$ qunta.sec^{-1} /1.02×10^{15} quanta·sec^{-1} = 14.5%

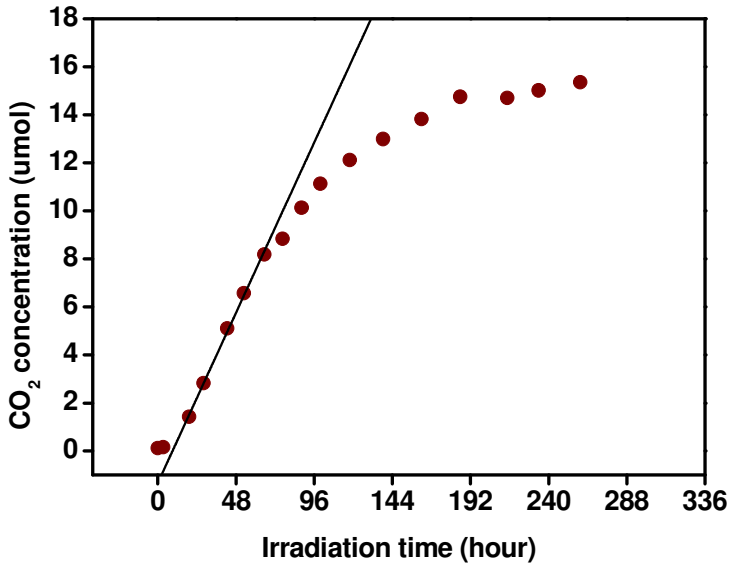

Figure S9. The CO_2 generation curve over Cu(II)-$(Sr_{1-y}Na_y)(Ti_{1-x}Mo_x)O_3$ at x = 2.0% under visible light irradiation. The CO_2 generation rate (R_{CO_2}) was obtained from the slope of the CO_2 generation curve between the irradiation time of ca. 10 to 70 h.